

Wind–Evaporation Feedback and the Axisymmetric Transition to Angular Momentum–Conserving Hadley Flow

WILLIAM R. BOOS AND KERRY A. EMANUEL

Program in Atmospheres, Oceans, and Climate, Massachusetts Institute of Technology, Cambridge, Massachusetts

(Manuscript received 19 March 2008, in final form 15 June 2008)

ABSTRACT

The effect of wind-induced surface heat exchange (WISHE) on axisymmetric, solstitial Hadley circulations is examined for forcings strong enough to produce meridional flow that nearly conserves absolute angular momentum in the free troposphere. Such forcings are known to produce an off-equatorial ascent zone in the summer hemisphere where the convergence of zonal momentum is balanced by drag on surface westerlies. Here, a convective quasi-equilibrium model with two vertical modes is used to show that enhanced surface entropy fluxes induced by these westerlies can intensify and shift both this ascent zone and the subcloud-layer entropy peak toward the equator. The equatorward shift of the subcloud entropy peak is associated with a reduction in the forcing amplitude needed to produce angular momentum–conserving (AMC) meridional flow. A previous theory of frontogenesis in tropical cyclones is adapted to axisymmetric Hadley circulations to show how WISHE shifts the peak subcloud entropy toward the equator.

These effects also occur for forcings that vary in a seasonal cycle, with the precise effect of WISHE depending on the peak amplitude of the forcing. For weak seasonally varying forcings, WISHE can abruptly increase the intensity of a local, viscous circulation, whereas for forcings of intermediate strength WISHE produces a transition to AMC flow when such a transition would not otherwise occur. For the strongest forcings, WISHE shifts the transition to AMC flow to a time earlier in the seasonal cycle. The possible relevance of these results to monsoon dynamics is discussed, as are possible effects of processes not represented in these axisymmetric models.

1. Introduction

The dynamical response to a zonally symmetric thermal forcing has been examined in a number of studies with the aim of understanding the dominant features of the earth's tropical and subtropical tropospheric circulation. These studies have used models that are axisymmetric (e.g., Held and Hou 1980; Lindzen and Hou 1988) as well as models that resolve eddy transports of heat and momentum (e.g., Walker and Schneider 2006). Strong thermal forcings with maxima positioned sufficiently far from the equator prove to be a special case in both types of models, because such forcings produce cross-equatorial flow that approximately conserves absolute angular momentum in the free troposphere. In axisymmetric models, the circulation shifts between this nonlinear, angular momentum–conserving (AMC) re-

gime and a nearly linear regime in which angular momentum advection is balanced by viscous damping (Plumb and Hou 1992). In eddy-resolving models, the circulation transitions between the nonlinear AMC regime and a regime in which angular momentum advection is balanced by the divergence of eddy momentum fluxes (Walker and Schneider 2006; Schneider and Bordoni 2008).

All of the studies just referenced employed relaxation to a prescribed equilibrium temperature as the thermal forcing. In the earth's atmosphere, however, the thermal forcing results from surface fluxes of sensible and latent heat that are redistributed by both convection and the large-scale circulation, with radiant emission to space serving as the final energy sink. The fact that these surface heat fluxes depend on wind speed can render the effective thermal forcing dependent on the circulation itself. Previous studies have examined certain aspects of the role played by wind-induced surface heat exchange (WISHE) in Hadley circulation dynamics (e.g., Numaguti 1995), but none has explored how WISHE might affect the transition to an

Corresponding author address: William R. Boos, Massachusetts Institute of Technology, Room 54–1721, 77 Massachusetts Ave., Cambridge, MA 02139.
E-mail: billboos@alum.mit.edu

AMC circulation. We showed in a previous work that a wind–evaporation feedback in axisymmetric (latitude–height) aquaplanet models can produce seasonal transitions of the Hadley circulation that are rapid compared to the time evolution of an imposed sea surface temperature (SST) forcing (Boos and Emanuel 2008, hereafter BE08). Study of this feedback was purposely limited to weak SST forcings that did not produce an AMC circulation to demonstrate that this particular WISHE mechanism is fundamentally different from the transition to an AMC state. However, thermal forcings on the earth may be stronger than the weak forcings examined by BE08, and it is entirely possible that WISHE may operate together with the transition to an AMC regime.

Here we examine how WISHE alters the dynamics of Hadley circulations driven by forcings sufficiently strong to produce an AMC response. The two-mode model described in BE08 is used for this task, both to reduce the computational burden of this exploration of parameter space and to allow for a simpler interpretation of results than would be possible with a primitive equation model. Fortunately, previous authors have already shown that two-mode models faithfully represent important aspects of the Hadley circulation dynamics, producing states with weak surface winds, strong upper-level winds, and approximate conservation of absolute angular momentum in the upper troposphere (Burns et al. 2006; Sobel and Neelin 2006).

Although the transition to an AMC state might be interesting in its own right, much of the practical motivation for studying this transition lies in the desire to explain the abrupt onset of monsoon circulations. A brief discussion of the abrupt nature of the onset of various monsoons was provided by BE08, and more extensive reviews of monsoon onset can be found in Webster et al. (1998), Wang (2006), and Lau and Waliser (2005). Here we simply note that the evolution of deep convection and horizontal wind in the South Asian and Australian monsoons occurs faster than can be explained by a linear response to the insolation forcing (e.g., Murakami et al. 1986; Krishnamurti et al. 1981).

The next section of this paper briefly reviews the numerical model and discusses some details of momentum conservation in this model. Then results are presented from a series of integrations using SST forcings of various strengths localized off the equator. One finding from these runs is that WISHE shifts the off-equatorial ascent zone toward the equator and reduces the forcing threshold needed to produce AMC flow. The mechanism responsible for this effect is discussed. Results for SST forcings with a nonzero cross-equatorial

gradient are then presented to show that these effects of WISHE can operate off the equator even when supercritical forcings already exist in equatorial regions. The paper closes with a brief summary and some remarks on the potential relevance of these results to observed monsoons.

2. Model details

We employ the same two-mode model used by BE08 to study the interaction of WISHE with AMC dynamics. Here we provide only a conceptual summary of the model and highlight a few relevant details, referring the reader to BE08 for the full model equations and parameters.

The model is similar to the quasi-equilibrium tropical circulation model (QTCM) of Neelin and Zeng (2000) in that the momentum equations are written on an equatorial β plane and projected onto a barotropic and first baroclinic mode. Instead of temperature and humidity, however, the thermodynamics are written in terms of the subcloud-layer moist entropy s_b and the saturation moist entropy of the free troposphere s^* . The atmosphere is assumed to have a moist adiabatic temperature structure in which s^* is constant with height, which allows the baroclinic component of the height field to be written in terms of s^* :

$$\begin{aligned} \frac{\partial u}{\partial t} + v \frac{\partial u}{\partial y} + w \frac{\partial u}{\partial z} - \beta y v &= Fu, \quad \text{and} \\ \frac{\partial v}{\partial t} + v \frac{\partial v}{\partial y} + w \frac{\partial v}{\partial z} + \beta y u &= (T - \bar{T}) \frac{\partial s^*}{\partial y} - \frac{\partial}{\partial y} \Phi_0 + F_v \end{aligned} \tag{1}$$

Here, Φ_0 is the barotropic component of the geopotential, \bar{T} is the vertical mean tropospheric temperature, and the F terms represent both surface drag and diffusion. The symbols u , v , w , and T have their usual meanings and are all functions of height (i.e., these momentum equations have not yet been projected onto vertical modes).

The tendencies of s^* and s_b are

$$\frac{\partial s^*}{\partial t} + v \frac{\partial s^*}{\partial y} = -N^2(w - \epsilon M_c) - R + \kappa \frac{\partial^2 s^*}{\partial y^2} \quad \text{and} \tag{2}$$

$$\begin{aligned} H_b \left(\frac{\partial s_b}{\partial t} + v \frac{\partial s_b}{\partial y} \right) &= E + \min[0, (w_b - M_c)](s_b - s_m) \\ &\quad + H_b \kappa \frac{\partial^2 s_b}{\partial y^2}, \end{aligned} \tag{3}$$

where M_c is the net upward mass flux in convective clouds, H_b is the depth of the subcloud layer, w_b is the vertical velocity at the top of the subcloud layer averaged over clear and cloudy areas, ε is a bulk precipitation efficiency, E is the surface entropy flux, N^2 is a dry stratification, and R is the rate of radiative cooling, which is fixed at 1 K day^{-1} . A subcloud-layer quasi-equilibrium closure (Raymond 1995) is used to define an equilibrium convective mass flux that would provide a constant value of s_b at each particular model time step, and the actual mass flux M_c is relaxed toward this equilibrium value over a time scale of 3 h. As in BE08, rather than including a prognostic equation for the entropy just above the subcloud layer s_m , we specify this entropy to differ from s_b by the constant amount χ .

These conservation equations are projected onto a barotropic mode \mathbf{v}_0 and a first baroclinic mode \mathbf{v}_1 defined in terms of the temperature of a moist adiabat:

$$\mathbf{v} \equiv \mathbf{v}_0 + T' \mathbf{v}_1. \quad (4)$$

Here, T' is the temperature anomaly relative to a mass-weighted vertical mean \bar{T} , normalized by $\Delta T \equiv T_s - \bar{T}$, where T_s is the surface air temperature:

$$T' \equiv \frac{T - \bar{T}}{\Delta T}. \quad (5)$$

The first baroclinic mode was defined in terms of the temperature T' because the baroclinic component of the momentum Eqs. (1) was written using the same form and can thus be easily projected onto this mode. As in BE08, T' was calculated assuming a spatially and temporally uniform temperature of 296 K at 1000 hPa, a dry adiabat up to 900 hPa, and a moist pseudoadiabat from 900 to 150 hPa. This provides a vertical structure for the first baroclinic mode qualitatively similar to that used in the QTCM (e.g., Zeng et al. 2000). Again, the complete projected momentum equations are provided in BE08.

The lower boundary of the model is entirely oceanic with prescribed SST. As an idealization of the thermal forcing associated with an off-equatorial landmass in a monsoon climate, we first use the same SST profile employed by BE08, which is similar in meridional structure to the thermal forcing of Plumb and Hou (1992). Between the latitudes $\phi_0 - \Delta\phi$ and $\phi_0 + \Delta\phi$, the SST is given by

$$T_{\text{PH}} = T_0 + \theta_{\text{PH}} \frac{\pi}{2} \cos^2\left(\frac{\pi}{2} \frac{\phi - \phi_0}{\Delta\phi}\right). \quad (6)$$

Outside this range, T_{PH} is set to the constant T_0 . This provides a meridionally confined SST anomaly cen-

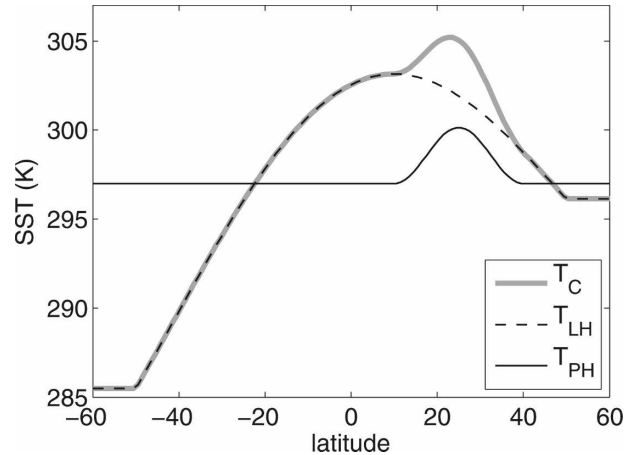


FIG. 1. SSTs used as forcings for the two-mode model. Analytic expressions for these distributions are given in the text. The solid black line shows T_{PH} and the dashed line shows T_{LH} . The solid gray line shows T_C , which is a combination of the two aforementioned profiles.

tered at ϕ_0 , with an amplitude set by θ_{PH} . We also examine the response to another SST distribution similar in meridional structure to the thermal forcing of Lindzen and Hou (1988), intended as an idealization of SST in the tropical ocean:

$$T_{\text{LH}} = T_1 - \theta_{\text{LH}}(\sin\phi - \sin\phi_1)^2. \quad (7)$$

This provides an SST that peaks at ϕ_1 and has a curvature that is nonzero everywhere in the tropics.

We will first examine the model response to T_{PH} , then to T_{LH} , and finally to a combination of the two obtained by the sum

$$T_C = T_{\text{PH}} + T_{\text{LH}} - T_0. \quad (8)$$

This forcing is intended as an idealization of the combined thermal effects of both an off-equatorial landmass and meridional gradients of oceanic SST, analogous to those found in South Asian longitudes. These three SST profiles are illustrated in Fig. 1 for $T_0 = 297 \text{ K}$, $\theta_{\text{PH}} = 2 \text{ K}$, $\phi_0 = 25^\circ\text{N}$, $\Delta\phi = 15^\circ$, $T_1 = 303.15 \text{ K}$, $\theta_{\text{LH}} = 20 \text{ K}$, and $\phi_1 = 10^\circ\text{N}$. It should be noted that our use of prescribed SST may produce an overactive WISHE feedback because, when the ocean mixed layer energy budget is taken into account, SSTs will be reduced in regions of high surface wind by enhanced surface enthalpy fluxes and increased entrainment of cold thermocline waters. On the other hand, wind-driven currents in a dynamical ocean would produce heat transports that might amplify, damp, or phase shift the WISHE response. Our use of prescribed SST is only intended as a first step in investigating the effects of WISHE.

For most integrations presented here, a surface gustiness of $v_g = 4 \text{ m s}^{-1}$ is used in the bulk formula for the surface entropy flux E :

$$E = \rho C_k |\mathbf{V}| (s_o^* - s_b), \quad \text{with}$$

$$\mathbf{V} = \sqrt{u^2 + v^2 + v_g^2}, \quad (9)$$

where s_o^* is the saturation entropy corresponding to the prescribed SST, C_k is a nondimensional transfer coefficient, ρ is the density of near-surface air, and u and v are the near-surface wind speeds. The model results are highly sensitive to v_g , as might be expected for solutions in which WISHE plays an important role. The particular value of $v_g = 4 \text{ m s}^{-1}$ was chosen mainly because it is near the smallest value for which solutions without intraseasonal transients were typically obtained; even with this value of v_g , some form of these transients does occur for some of the stronger forcings presented here. As discussed in BE08, solutions which contain such transients may be relevant to observed monsoon behavior but will be explored in separate work. In addition to suppressing intraseasonal transients, use of a high value for v_g is also expected to damp the positive feedback of WISHE on the seasonal cycle of meridional flow, an effect qualitatively opposite to that produced by our neglect of ocean mixed layer coupling.

Except for the runs with seasonally varying forcings, all model results presented here are diagnostics taken after the model reached a steady state, which typically happened within 50 days of simulated time.

Angular momentum conservation

The conserved quantity

$$m \equiv u - \beta y^2/2 \quad (10)$$

is the analog of absolute angular momentum on an axisymmetric β plane with meridional coordinate y , and hereafter we use absolute angular momentum synonymously with m . Burns et al. (2006) showed that two-mode models approximately conserve m only at one particular level near the tropopause. Following their analysis, an expression for m conservation in our two-mode model can be obtained by combining the conservation equations for the barotropic and baroclinic modes of zonal wind (u_0 and u_1 , respectively) to eliminate the quantity $u_1 \partial_y v_1$:

$$v_1 \left[\frac{\partial}{\partial y} (u_0 + Au_1) - \beta y \right] = -B \frac{C_D |\mathbf{V}|}{H} (u_0 + u_1). \quad (11)$$

Here, v_1 is the baroclinic mode of meridional wind, C_D is a nondimensional drag coefficient, and H is the pre-

TABLE 1. Parameters used in the two-mode model. Only parameters referred to in the text are included; the complete model parameter set is given in BE08.

Parameter name	Symbol	Value
Surface minus mean atmospheric temperature	ΔT	35 K
Mean boundary layer depth	H_b	910 m
Mean tropopause height	H	14 km
Dry static stability	N^2	$1.0 \text{ J kg}^{-1} \text{ m}^{-1}$
Normalized second moment of temperature	$\langle T'^2 \rangle$	0.57
Normalized third moment of temperature	$\langle T'^3 \rangle$	-0.36
Correlation function for vertical advection	$\langle \Omega T' \partial_p T' \rangle$	-0.18
Surface transfer coefficient for momentum	C_D	0.0012
Enthalpy exchange coefficient	C_κ	0.0012
Surface gustiness	v_g	4.0 m s^{-1}
Radiative cooling rate	\bar{R}	1 K day^{-1}
Bulk precipitation efficiency	ε	0.85
Entropy drop at top of subcloud layer (χ)	$\theta_{eb} - \theta_m$	15 K
Gradient of Coriolis parameter	β	$2.28 \times 10^{-11} \text{ m}^{-1} \text{ s}^{-1}$
Specific heat of air at constant pressure	c_p	$1010 \text{ J kg}^{-1} \text{ K}^{-1}$

scribed depth of the troposphere. The quantities A and B are combinations of constants dependent on the particular vertical structure assumed for the baroclinic mode:

$$A = \frac{\langle T'^3 \rangle}{\langle T'^2 \rangle} + \frac{\langle \Omega T' \partial_p T' \rangle}{\langle T'^2 \rangle} \quad \text{and}$$

$$B = \frac{\langle \Omega T' \partial_p T' \rangle}{\langle T'^2 \rangle^2} + \frac{1}{\langle T'^2 \rangle}. \quad (12)$$

Here, angled brackets denote mass-weighted vertical integrals through the depth of the troposphere and Ω is the vertical structure of the vertical velocity field. The individual terms in (12) were derived in BE08 and their values are listed in Table 1.

Burns et al. (2006) derived asymptotic solutions to the two-mode QTCM of Neelin and Zeng (2000) in terms of a small parameter that is the ratio of the meridional advective terms to surface drag terms in the momentum equations. To first order in this parameter, they showed that m conservation holds only at one particular level near the tropopause and that the surface drag that would violate angular momentum conservation has a magnitude one order smaller; that is, to first order, the right-hand side of (11) is zero. Then, in the presence of nonzero meridional flow, the absolute vor-

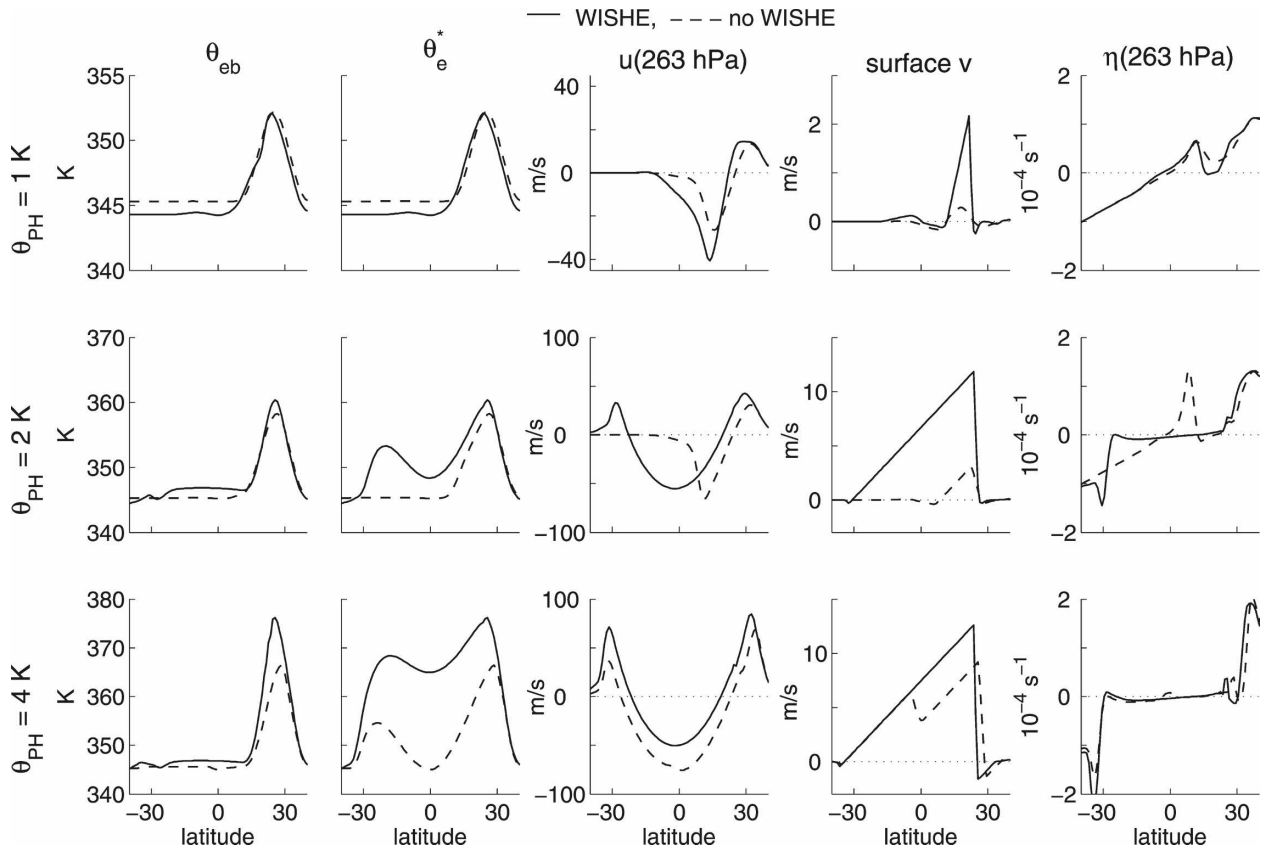


FIG. 2. The equilibrated response of the two-mode model to steady T_{PH} forcings of three different amplitudes. Solid lines show results from runs with wind-dependent surface entropy fluxes (with WISHE), and dashed lines indicate runs with wind-independent surface entropy fluxes (no WISHE). Each row shows the response to a given forcing, with the amplitude of θ_{PH} in Eq. (6) displayed on the left. From left to right, the columns show the subcloud-layer equivalent potential temperature, the saturation equivalent potential temperature of the free troposphere, the zonal wind near the model tropopause, the surface meridional wind, and the absolute vorticity near the tropopause.

ticity will vanish to first order only at the particular level where

$$T' = A. \quad (13)$$

This is 263 hPa for the parameters used in our two-mode model, which is 113 hPa below the specified tropopause. In the diagnostics presented below, the degree of angular momentum conservation is therefore assessed using the absolute vorticity η at 263 hPa.

3. Results for subtropical forcing

This section presents the model response to the T_{PH} forcing, in which the SST peaks in the subtropics and has no gradient or curvature on the equator. The first two parts of this section present the model response to steady forcings of three different magnitudes, with θ_{PH} in (6) set to 1, 2, and 4 K. The response to the forcing with $\theta_{\text{PH}} = 1$ K was examined in a seasonally varying

configuration by BE08. The last part of this section examines the effect of WISHE for a seasonally varying version of the same T_{PH} forcing, but with a higher amplitude of $\theta_{\text{PH}} = 5$ K.

a. Steady forcing without WISHE

The model is first integrated with $|\mathbf{V}|$ in the bulk surface flux Eq. (9) set to a constant value of 6 m s^{-1} everywhere. The value of 6 m s^{-1} for $|\mathbf{V}|$ is the same as that used by BE08 for runs without WISHE and provides a value that exceeds the specified surface gustiness of 4 m s^{-1} . These integrations are henceforth referred to as the “no-WISHE” runs.

For these no-WISHE runs with θ_{PH} set to 1 and 2 K, the meridional circulation is almost entirely confined to the summer hemisphere, and the strength of this circulation increases with the magnitude of the forcing (Fig. 2, dashed lines in top two rows). Absolute angular momentum is not homogenized meridionally in the upper

troposphere, as indicated by the nonzero values of η in this region. The entire domain is convecting, as indicated by the fact that s^* is nowhere greater than s_b (in all figures, entropies are expressed in temperature units, using the definitions $s^* \equiv c_p \ln \theta_e^*$ and $s_b \equiv c_p \ln \theta_{eb}$).

In contrast, for the run with $\theta_{\text{PH}} = 4$ K, a strong meridional circulation extends from about 40°S to 25°N , with upper-level m nearly homogenized within 20° of the equator (Fig. 2, dashed line in bottom row). The absolute vorticity deviates slightly from zero near the equator, where a secondary ascent zone exists (ascent can be inferred directly from surface v because the meridional wind has a purely first baroclinic mode structure). This secondary ascent zone occurs on the winter side of the equator, and we discuss in appendix A how it seems to result from the mechanism discussed by Pauluis (2004), in which surface drag inhibits cross-equatorial flow from occurring within the boundary layer. Deep convection in this no-WISHE run is suppressed in the Southern Hemisphere, where subsidence occurs and where $s^* > s_b$. The meridional structure of this solution is generally consistent with previous theories of solstitial, axisymmetric AMC circulations (e.g., Lindzen and Hou 1988; Plumb and Hou 1992), and here we discuss a few relevant features. Near the tropopause, the zonal wind is constrained by m conservation to vary quadratically with latitude, which is roughly the structure seen in the model results. The s^* distribution has the equatorial minimum and off-equatorial maxima characteristic of m conservation. Where convection is suppressed, free-tropospheric temperatures are maintained by a balance between subsidence warming and radiative cooling, which when combined with the axisymmetric continuity equation shows that v must increase linearly with latitude:

$$\frac{\partial v}{\partial y} = \frac{R}{N^2 H}. \quad (14)$$

For the parameters of the two-mode model, which include fixed values of radiative cooling, static stability, and tropopause height, this produces a surface wind v_1 that increases by about 2 m s^{-1} for every 10° of latitude, consistent with what is seen in the convectively stable region.

Peak meridional winds for the run with $\theta_{\text{PH}} = 4$ K are several times larger than the peak observed zonal mean meridional wind during boreal summer (e.g., Peixoto and Oort 1992), but this does not necessarily indicate a deficiency in the numerical model. The wind profile is at least roughly consistent with the axisymmetric general circulation model (GCM) used in BE08, in which peak meridional winds of 8 m s^{-1} were obtained for a

forcing of similar amplitude. Perhaps meridional winds are weaker in observations because some process not represented in these axisymmetric models causes ascent on the earth to occur over a broader range of latitudes. Alternatively, the SST forcing in the model might be considerably stronger than the relevant thermal forcings achieved on the earth; it is difficult to compare these forcings directly because we are using an SST anomaly as a proxy for a land surface thermal forcing.

b. Steady forcing with WISHE

Now we examine the model response when surface entropy fluxes are allowed to depend on wind speed according to (9). A series of integrations is presented with the same forcings used in the no-WISHE runs, with θ_{PH} set to 1, 2, and 4 K. The response to the weakest forcing, with an amplitude of 1 K, is a viscously dominated circulation localized in the summer hemisphere with little meridional homogenization of m (Fig. 2, solid lines in top row). The circulation is similar in structure to that obtained for the no-WISHE run using the same SST, but WISHE increases the peak meridional flow by almost an order of magnitude. The mechanism by which WISHE enhances this flow is discussed in detail in BE08.

For the slightly stronger forcing of $\theta_{\text{PH}} = 2$ K, the circulation enters an AMC regime with the classic structure of a single off-equatorial convergence zone in the summer hemisphere, a bimodal distribution of s^* , and a broad region of subsidence stretching across the equator well into the winter hemisphere (Fig. 2, solid lines in second row). For the run without WISHE, the 2-K forcing did not produce an AMC circulation, so WISHE effectively reduces the critical amplitude of the SST forcing needed to produce AMC flow. Comparison of the profiles of subcloud-layer entropy for the two runs with $\theta_{\text{PH}} = 2$ K shows that WISHE narrows the s_b peak, increases its amplitude, and shifts it toward the equator (Fig. 3). Also plotted in Fig. 3 are the corresponding critical distributions of subcloud entropy; in the inviscid limit, AMC meridional flow must occur when the s_b curvature exceeds that of the critical distribution. Such critical distributions were originally calculated for free-tropospheric temperature by Plumb and Hou (1992), rephrased in terms of the subcloud entropy distribution by Emanuel (1995), and then adapted to the two-mode model in appendix B. The subcloud entropy is nowhere supercritical in the no-WISHE run, whereas it is supercritical in the run with WISHE, with the departure of subcloud-layer θ_e from the critical distribution peaking at about 3 K at near 15°N . Thus, although the effects of WISHE on the subcloud entropy peak may seem small in amplitude, they

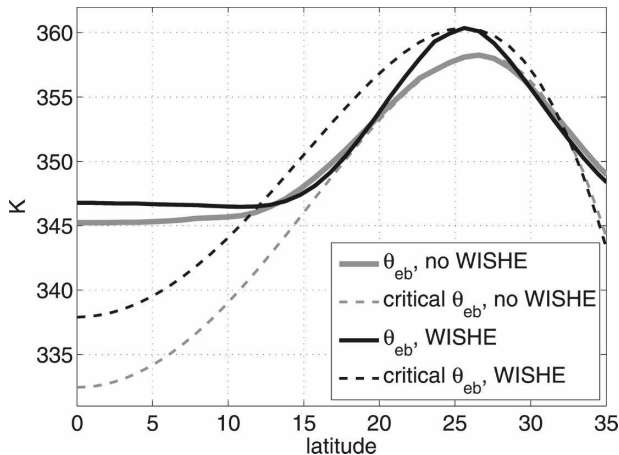


FIG. 3. Subcloud-layer equivalent potential temperature (solid lines) and the critical distribution of the same quantity (dashed lines). All quantities are for the equilibrated response to the steady T_{PH} forcing with $\theta_{\text{PH}} = 2$ K. Gray lines denote results for the no-WISHE run; black lines indicate the run with WISHE.

are sufficient to shift the circulation into an AMC regime. The shift to supercriticality seems to be associated with both an increase in the amplitude of the s_b peak and a shift of the peak toward the equator, either of which could shift the entropy distribution into supercriticality.

The increase in amplitude of the s_b peak in the run with WISHE is consistent with the larger peak surface enthalpy fluxes seen in that run, if one assumes that the negative tendency of s_b due to convection will not entirely compensate for the positive tendency due to increased surface enthalpy fluxes (Fig. 4). This is suggestive of the positive feedback between the meridional gradient of surface enthalpy fluxes and the strength of the Hadley circulation, as discussed by BE08. Here, that feedback may simply have become large enough to cause a transition to an AMC state, although such an explanation does not account for the equatorward shift of the s_b peak, which will be discussed in greater detail below. Surface enthalpy fluxes in the two-mode model are quite small in regions outside the Hadley circulation, falling to a minimum of about 35 W m^{-2} . Such low values seem to occur because surface entropy fluxes in this model are balanced primarily by the compensating subsidence between cumulus clouds that advects dry lower-tropospheric air downward from just above the subcloud layer, whereas the downward transport by unsaturated downdrafts of even drier air from the midtroposphere is not represented. This results in the subcloud layer in the two-mode model having a specific entropy much closer to that of the underlying sea surface than the near-surface air in, say, the QTCM or the primitive equation model used in BE08. Although this

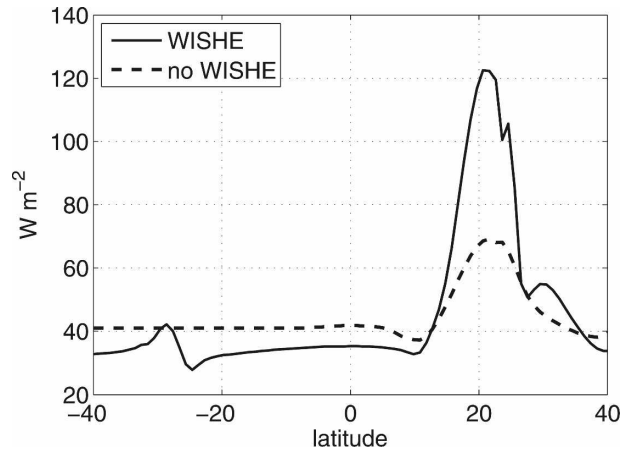


FIG. 4. As in Fig. 3, but showing the surface enthalpy flux. Note the change in horizontal scale compared to Fig. 3.

may be a notable deficiency in this model, it nevertheless exhibits WISHE feedbacks on the Hadley circulation similar to those seen in a primitive equation model (this similarity was shown by BE08 for weak forcings and is discussed below for stronger forcings).

For the stronger forcing of $\theta_{\text{PH}} = 4$ K, an AMC circulation is also produced (Fig. 2, solid lines in bottom row). The main differences compared to the circulation achieved for the weaker forcing of $\theta_{\text{PH}} = 2$ K are a slight poleward expansion of the cross-equatorial Hadley cell in the winter hemisphere, a considerably larger s_b peak, and a distribution of free-tropospheric s^* that is shifted nearly uniformly to higher values over the entire Hadley circulation. As noted above, turning off WISHE has several effects: a secondary ascent zone is produced just south of the equator, the ascent zone near 25°N shifts slightly poleward, and upper tropospheric winds become more easterly within the bounds of the cross-equatorial Hadley cell. The existence of the near-equatorial ascent zone for the no-WISHE run is sensitive to the value prescribed for $|\mathbf{V}|$; increasing this value from the default value of 6 to 10 m s^{-1} produces a single ascent zone near 25°N with uniform subsidence everywhere else within the cross-equatorial Hadley cell (as seen in the surface divergence field shown in Fig. 5, dashed line in top panel).

One persistent feature of these model runs is that WISHE shifts the s_b peak and the ascent zone slightly toward the equator. These quantities are expected to move together because the maximum ascent is constrained to occur slightly equatorward of the maxima in s_b and free-tropospheric temperature (e.g., Privé and Plumb 2007; Emanuel 1995). On the one hand, these meridional shifts in the s_b peak and the ascent zone seem fairly minor, suggesting that m conservation pro-

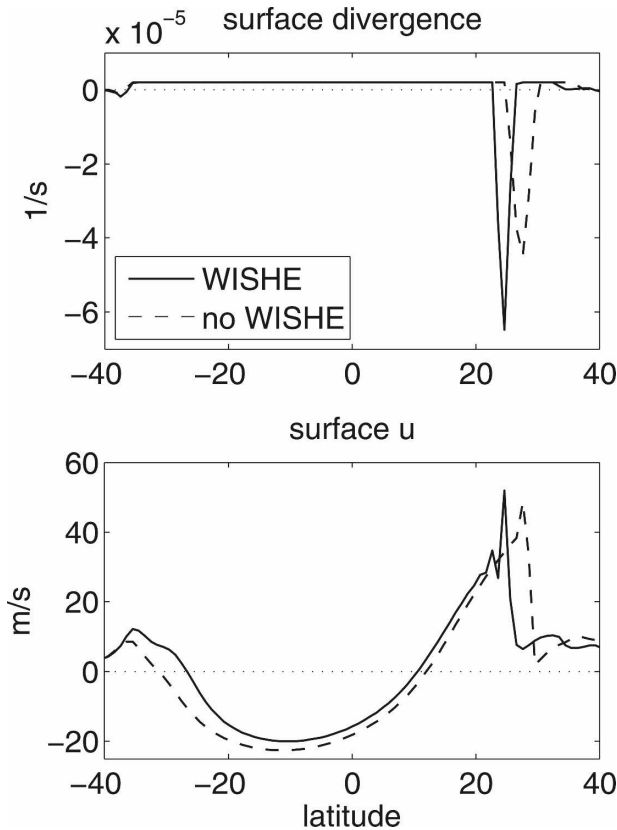


FIG. 5. (top) Divergence of the surface horizontal wind (i.e., $\partial_y v_i$) and (bottom) total surface zonal wind, both for the equilibrated two-mode model with $\theta_{PH} = 4$ K. Solid lines denote results for run with WISHE; dashed lines indicate the no-WISHE run, with $|\mathbf{V}|$ in the bulk flux formula set to 10 m s^{-1} .

vides a strong constraint that limits the dynamical effect WISHE can have for strong SST forcings. However, given that axisymmetric Hadley circulations can be quite sensitive to small meridional shifts in the thermal maximum (Lindzen and Hou 1988) and that an equatorward shift in the s_b peak is associated with a reduction in the forcing strength needed to achieve AMC flow (Emanuel 1995), we believe these meridional shifts merit closer inspection. For $\theta_{PH} = 4$ K, the ascent zone in the run with WISHE is centered about 3° farther south and is narrower and more intense than in the run without WISHE (Fig. 5, top panel). Although this meridional shift of the ascent zone may seem small, zonal winds within the bounds of the AMC circulation are highly sensitive to the latitude of ascent. If, as in previous axisymmetric theory (Held and Hou 1980; Lindzen and Hou 1988), ascent is assumed to occur entirely at one latitude ϕ_0 where horizontal winds are zero, and if upper-level flow in the cross-equatorial branch of the circulation is assumed to strictly conserve m , then a shift in ϕ_0 from 26° to 23° will make upper-

level zonal winds more westerly by about 20 m s^{-1} . This is consistent with the difference in upper tropospheric winds seen in the runs with and without WISHE for $\theta_{PH} = 4$ K (Fig. 2, bottom row).

The mechanism by which WISHE accomplishes this meridional shift in the ascent zone and the s_b peak will be discussed in the next section, but we make a few diagnostic comments here. WISHE can be expected to increase vertical velocities in the ascent zone because large surface wind speeds enhance surface enthalpy fluxes there. The direct relationship between surface enthalpy fluxes and ascent can be seen explicitly in the two-mode model by rearranging the steady-state version of the budget for s^* , given in (2), under the assumption of strict subcloud-layer equilibrium:

$$w = \frac{1}{1 - \varepsilon} \left(\varepsilon C_k |\mathbf{V}| \frac{s_o^* - s_b}{\chi} - \frac{R}{N^2} \right). \quad (15)$$

This denotes a balance between radiative cooling, adiabatic warming (by the subsidence needed to balance any net upward convective mass flux), and adiabatic cooling (due to any large-scale vertical velocity). Because R , N^2 , ε , and χ are constant in this model, w can be expected to increase with $|\mathbf{V}|$. For solstitial AMC circulations, surface westerlies must exist in the ascent zone for surface drag to balance the convergence of zonal momentum into this region (as discussed by Lindzen and Hou 1988). In the two-mode model with $\theta_{PH} = 4$ K, these surface westerlies peak near 40 m s^{-1} (Fig. 5), so that runs with WISHE easily have stronger surface entropy fluxes than no-WISHE runs. These peak surface westerlies are about twice as strong as those observed near the ascent zone in the South Asian summer monsoon (e.g., Halpern and Woiceshyn 1999), which could be due either to the use of an SST forcing somewhat stronger than that needed to represent typical monsoon forcings on the earth or to some other process not represented in this simple model. In particular, the lack of a prognostic boundary layer in the model surely has some effect on surface wind speeds. But the absolute magnitude of surface zonal winds is somewhat of a side issue, because as long as the surface wind speed is larger than the surface gustiness v_g (a condition easily met by typical monsoonal westerlies in observations), WISHE can be expected to enhance vertical velocities in the ascent zone in a state of subcloud-layer quasi-equilibrium.

The fact that the increase in vertical velocities in the ascent zone is accompanied by a narrowing of that zone is consistent with the conservation of mass. That is, if the magnitude of subsidence is bounded by radiative cooling, and the meridional extent of the subsiding re-

gion is not considerably modified by WISHE, as is the case in these integrations, then mass conservation dictates that the ascent zone must narrow as its upward velocities increase.

As noted in the previous section, the use of prescribed SST may produce an overactive WISHE feedback because SST is expected to be reduced in regions of high surface wind speed. One piece of evidence for such an overactive feedback would be a large increase in the domain-mean surface enthalpy flux in runs with WISHE. For the forcing with $\theta_{\text{PH}} = 2$ K, the domain mean surface enthalpy flux differs by less than 5% between WISHE and no-WISHE runs because the surface wind speed prescribed in the no-WISHE run is quite close to the global mean surface wind speed in the WISHE run. For stronger forcings, however, the difference in domain-mean surface enthalpy flux is considerably larger and thus indicative of regimes in which damping due to interactive SST might play an important role. The domain-mean surface fluxes also depend on the value chosen for the surface gustiness v_g , which in this study was set to be high enough to provide some damping on WISHE feedbacks, as discussed in the previous section.

Although adding an ocean mixed layer of uniform depth to our axisymmetric models might be seen as one simple way of assessing the effect of interactive SST, we expect large horizontal gradients in surface thermal inertia to be necessary for sustaining a strong WISHE feedback on solstitial Hadley flow. Without such large gradients, a strong seasonal cycle in the Hadley circulation will be achieved only for shallow mixed layers, but WISHE will be largely eliminated for surfaces with such small heat capacities. In other words, monsoons are traditionally thought to exist because a land surface with a low heat capacity lies poleward of an ocean surface with a large heat capacity, and we expect such a configuration to be necessary for assessing the effects of interactive SST on WISHE in the Hadley circulation. This task is left for future work.

c. Seasonally varying forcing

How does WISHE alter the seasonal cycle of the Hadley circulation when the time-dependent SST forcing reaches sufficient amplitude to produce AMC flow? To answer this question, we integrated the two-mode model with an SST prescribed to vary in a seasonal cycle:

$$T_{\text{PH,seas}} = T_0 + \theta_{\text{PH}} \frac{\pi}{2} \cos\left(2\pi \frac{t}{365 \text{ days}}\right) \times \cos^2\left(\frac{\pi \phi - \phi_0}{2 \Delta\phi}\right). \quad (16)$$

This has the same meridional structure as the T_{PH} forcing, but the amplitude of the off-equatorial SST anomaly varies in a seasonal cycle. This seasonal cycle is a full sinusoid in that the off-equatorial anomaly is negative during “winter” and is the same cyclic SST forcing used in BE08 but with a larger peak amplitude. Here we use a peak amplitude of $\theta_{\text{PH}} = 5$ K, which for steady forcings produces AMC flow with a single ascent zone near ϕ_0 even in the absence of WISHE (not shown). The amplitude of the off-equatorial forcing was varied, rather than the latitude of the forcing’s peak, to provide an idealization of the solar forcing incident on a subtropical landmass in a monsoon climate. Variations in near-equatorial SST may also play an important role in monsoon dynamics and are considered in a later section of this paper.

To assess the linearity of the model response, we use a quantity defined in BE08 as the PBL flow, which is the meridional mass flux integrated both vertically through the lowest 200 hPa of the atmosphere and meridionally over all latitudes. The PBL flow provides a measure of the net mass flux in the Hadley circulation; equatorially antisymmetric flow makes no contribution to this metric, by design. The PBL flow is plotted against the SST at 25°N to produce a phase diagram, which shows that an abrupt increase in the sensitivity of meridional flow to SST occurs in runs both with and without WISHE (as indicated by the arrows in the left panel of Fig. 6). Here WISHE was turned off by specifying $|\mathbf{V}| = 6 \text{ m s}^{-1}$, as for most of the runs with steady forcing. As discussed in BE08, the trajectory in this phase space would be an ellipse for a purely linear response to the SST forcing; the increase in the slope of the trajectory that occurs after the off-equatorial SST anomaly becomes positive corresponds to an abrupt intensification of the solstitial Hadley flow. This intensification does occur simultaneously with a transition to an AMC state in which η is approximately zero near the model tropopause (not shown). The effects of WISHE are to shift this onset of AMC flow to a time earlier in the season, to shift the withdrawal of that flow to a time later in the season, and to produce subseasonal oscillations in the strength of the flow during summer. The fact that the onset of AMC flow occurs earlier in the year for runs with WISHE is consistent with the finding that, for the runs with steady forcing, WISHE reduced the amplitude of the SST forcing needed to achieve an AMC state. The oscillations that occur after onset have a period of roughly 15 days and seem to exhibit stationary growth and decay rather than meridional propagation (not shown). Thus, although these subseasonal transients require WISHE for their existence, they are decidedly different from the meridionally propagating

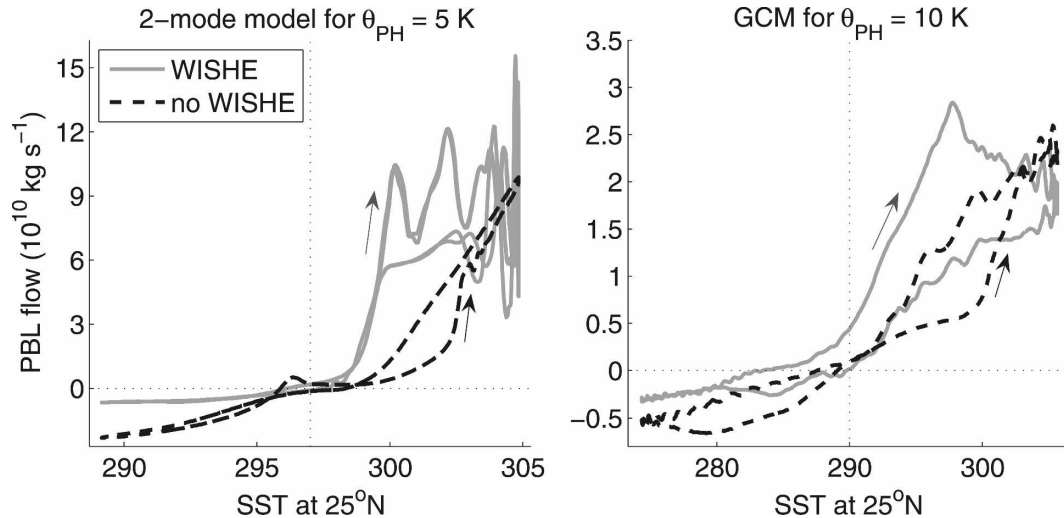


FIG. 6. The PBL flow plotted against the SST at 25°N for the seasonally varying version of the subtropical forcing. Phase diagrams for (left) the two-mode model with $\theta_{\text{PH}} = 5\text{ K}$ and (right) the primitive equation model for $\theta_{\text{PH}} = 10\text{ K}$. Solid gray lines denote results for runs with WISHE; dashed black lines indicate no-WISHE runs. Time progresses in the direction shown by the arrows, which are positioned near the time of transition to AMC flow.

modes found by Bellon and Sobel (2008), which also required WISHE for their instability. Propagating intraseasonal transients are observed in monsoon circulations (e.g., Yasunari 1979), and their role in the seasonal cycle of Hadley flow merits further attention in separate work.

These results show that for a seasonally varying SST forcing sufficiently strong to produce AMC flow even if surface entropy fluxes did not depend on wind speed, WISHE has the effect of shifting the transition to AMC flow to a time earlier in the seasonal cycle. For much weaker SST forcings, BE08 showed that WISHE could produce a nonlinear intensification of solstitial flow even though an AMC state was never achieved. We do not show the phase diagram for the intermediate case where AMC flow would occur only with WISHE because its individual trajectories resemble those for the other cases: the trajectory for the run with WISHE is similar to that for the strong forcing displayed in Fig. 6, whereas the trajectory for the run without WISHE is an approximate ellipse with much weaker peak meridional flow, similar to those shown in BE08. A later section of this paper does examine a seasonally varying version of the combined forcing T_C for which WISHE is needed to produce AMC flow that originates from an ascent zone near the subtropical forcing.

The response to seasonally varying SST of the form given by (16) was also examined in the primitive equation model discussed in BE08. This model, described by Pauluis and Emanuel (2004), is an axisymmetric atmospheric version of the Massachusetts Institute of Tech-

nology (MIT) GCM with parameterizations of moist convection, radiation, and other subgrid-scale processes. Phase trajectories of PBL flow in this model also show that WISHE shifts the abrupt onset of summer flow to an earlier time in the seasonal cycle (Fig. 6, right panel). Compared to the two-mode model, the onset was less abrupt in the GCM. Also, a higher-amplitude forcing was needed to produce an abrupt onset in the absence of WISHE in the GCM, which is why we present results for $\theta_{\text{PH}} = 10\text{ K}$, which is double the forcing amplitude used in the seasonal run of the two-mode model (T_0 was also reduced by $5\pi/2$ to avoid prescribing SSTs considerably higher than those observed on the earth). The reduction due to WISHE of the critical forcing amplitude was thus even stronger in the GCM than in the two-mode model. The GCM produced only about one-third the PBL flow of the two-mode model during peak summer, seemingly because for such strong forcings a larger fraction of the northward mass flux occurs above the boundary layer due to the equatorial jumping effect described by Pauluis (2004). The equilibrated response to steady subtropical forcings was not explored in the GCM.

4. Moist frontogenesis

The previous section showed that although m conservation constrains the dynamics of the Hadley circulation for sufficiently strong SST forcings, WISHE can alter the response in nontrivial ways. In particular, WISHE reduced the critical forcing amplitude needed

to achieve AMC flow by producing a narrowing, intensification, and equatorward shift of both the s_b peak and the ascent zone. This section attempts to explain these effects using an adaptation of a previous theory of eyewall frontogenesis for tropical cyclones (Emanuel 1997, hereafter E97). A heuristic discussion of this theory is presented first, followed by a more detailed analytical treatment.

a. Heuristic discussion

E97 showed that WISHE and the horizontal advection of subcloud-layer entropy can create sharp radial gradients in azimuthal wind in an axisymmetric tropical cyclone, thereby forming the storm eyewall. It might seem reasonable to expect that a similar frontogenetic mechanism might operate in Hadley flow because Hadley circulations and tropical cyclones have both been idealized as axisymmetric balanced vortices, albeit with differences in some key parameters (e.g., Wirth and Dunkerton 2006).

To illustrate the frontogenetic effects of WISHE and s_b advection on the zonal wind field in the Hadley circulation, we begin by examining the idealized case of inviscid thermal wind balance and a convecting domain in strict subcloud-layer equilibrium. The linearized, steady meridional momentum balance and the linearized free-tropospheric temperature balance are then

$$\beta y u = (T - \bar{T}) \frac{\partial s^*}{\partial y} - \frac{\partial \Phi_0}{\partial y} \quad \text{and} \quad (17)$$

$$\frac{\partial s^*}{\partial t} = -N^2(1 - \varepsilon)w + \varepsilon N^2 C_k |\mathbf{V}| \frac{s_o^* - s_b}{\chi} - R. \quad (18)$$

These are height-dependent equations and have not been projected onto vertical modes. Suppose that a poleward gradient of s^* is imposed, that u is in thermal wind balance with this free-tropospheric temperature distribution, and that this state is maintained until time t , as shown in Fig. 7. Suppose also that after time t , the s^* distribution is allowed to be modified only by the term in (18) involving $|\mathbf{V}|$, and that meridional variations in $|\mathbf{V}|$ are proportional to variations in the baroclinic component of the zonal wind. The latter assumption is a weaker condition than neglecting the barotropic wind altogether and requires both that the total surface wind has the same sign as its baroclinic component and that the barotropic wind does not vary in such a way as to exactly cancel the effects discussed here. Given these assumptions, which are made more precise in the analytical treatment presented below, the WISHE tendency represented by the second term on the right-hand side of (18) will, after the lapse of a short

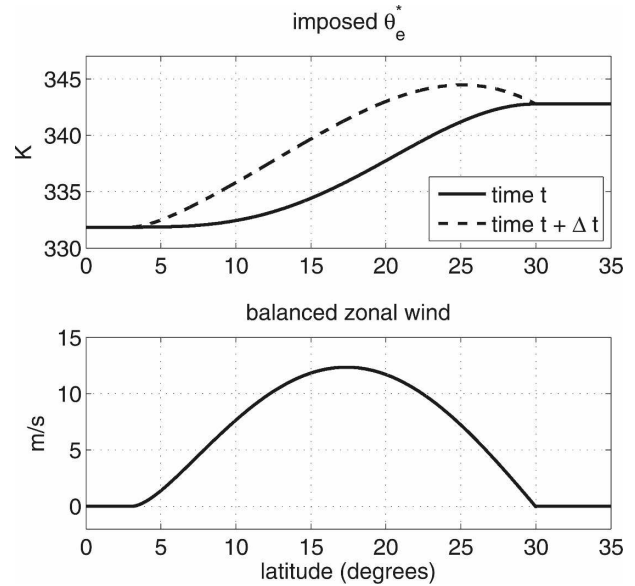


FIG. 7. Schematic of (top) an imposed distribution of free tropospheric saturation equivalent potential temperature (solid line) and (bottom) the baroclinic component of the surface zonal wind needed to achieve thermal wind balance on a β -plane. The dashed line in the top panel shows the change in θ_e^* due only to WISHE after some short time interval Δt . See text for details.

time interval Δt , increase s^* nonuniformly so that the maximum meridional gradient of s^* will increase, and both the peak s^* and its maximum gradient will shift toward the equator (as illustrated in Fig. 7). In other words, the peak heating will occur where the gradient in s^* is largest, which will shift the location of this maximum gradient toward the equator. Given a boundary condition of fixed s^* somewhere near the equator, this equatorward shift must be accompanied by an increase in magnitude of the s^* gradient.

If thermally direct meridional flow is assumed to exist in the presence of this s^* distribution and a quasi-equilibrium state exists with $s_b = s^*$, then a horizontal advective tendency will act on s_b ¹. This advective tendency will be negative within the region of thermally direct flow and so will increase the maximum gradient of s_b and shift it poleward (not shown). Although this argument concerns the advection by meridional flow in general, we note in the next section that it is the meridional flow induced by surface friction that actually leads to a frontogenetic effect (consistent with the results of E97).

¹ In the axisymmetric two-mode model, s^* cannot be directly modified by meridional advection because it is constant with height and v is purely baroclinic. Horizontal advection can alter s^* only indirectly by acting on s_b .

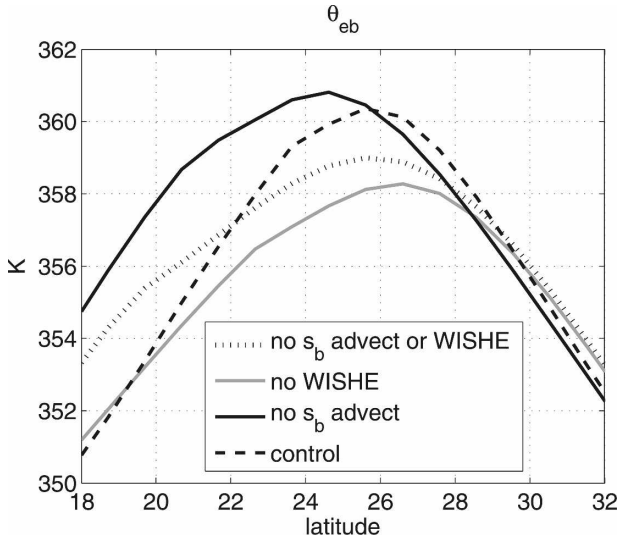


FIG. 8. Subcloud-layer equivalent potential temperature for the equilibrated response to the steady T_{PH} forcing with $\theta_{PH} = 2$ K. The dotted line shows the profile for a run without WISHE or horizontal advection of s_b ; the solid gray line, a run without WISHE but with s_b advection; the solid black line, a run with WISHE but without s_b advection; and the dashed line, a run with both WISHE and s_b advection.

The s_b distribution is thus altered by both WISHE and s_b advection, with WISHE shifting the peak gradient of s_b (and thus the peak zonal wind) toward the equator and advection shifting it toward the pole. Both processes enhance meridional entropy gradients. These qualitative hypotheses, treated in greater analytical detail below, are confirmed by repeating both the WISHE and no-WISHE runs of the two-mode model without horizontal advection of s_b (for the steady forcing with $\theta_{PH} = 2$ K). Advection of s_b was turned off simply by omitting the term $v_1 \partial_y s_b$ from the conservation equation for subcloud-layer entropy; although this produces a system that does not conserve the relevant analog of total energy, it proves useful as a process study. Results from these integrations confirm our previous statements: meridional advection generally shifts the s_b peak poleward, whereas WISHE shifts it toward the equator (Fig. 8). Together, these processes narrow and intensify the s_b peak. Because the ascent zone is expected to be located just equatorward of the s_b peak, similar meridional shifts are expected to occur in the ascent zone, consistent with results from the two-mode model.

We have thus far implicitly assumed that any frontogenetic tendency in the numerical model will be balanced by horizontal diffusion. This does seem to occur because the width of the ascent zone was reduced by a factor of 2 in a version of the model integrated (for $\theta_{PH} = 2$ K) with the horizontal diffusion coefficient κ_H

reduced from its default value of 1×10^5 to 5×10^3 $m^2 s^{-1}$ (not shown). This value of κ_H was near the smallest value for which numerically stable solutions could be obtained and required reducing the model grid spacing from 1.0° to 0.1° of latitude.

The above discussion, as well as the treatment below, assumes a convecting domain, and only a small part of the domain is convecting in the two-mode model for the stronger SST forcings. Nevertheless, it seems that these frontogenetic processes do operate in the relatively narrow region of ascent in the two-mode model. Physics arising from the discontinuities between convecting and nonconvecting regions is an active topic of research (e.g., Frierson et al. 2004) and is not explored further here.

b. Analytical treatment

Here we show analytically how discontinuities can be formed in the zonal velocity field under the condition of subcloud-layer quasi-equilibrium, following a treatment similar to that of hurricane eyewall frontogenesis put forth by E97, but on an axisymmetric β plane without the centrifugal terms important for tropical cyclones. Part of this frontogenetic process will be shown to occur because WISHE shifts the s_b peak toward the equator, but both horizontal advection of s_b and nonlinear momentum advection will also be shown to play a role. In this sense, the frontogenetic process discussed here is more general than the WISHE effects that were the focus of previous sections of this paper.

The analysis is performed using m , defined by (10), as a horizontal coordinate instead of y . This allows us to show that the nonlinear momentum advection that is part of m conservation accelerates the frontogenetic process and to more clearly understand the role played by s_b advection. Following E97, we define a coordinate transformation

$$\frac{\partial}{\partial y} = \frac{dm}{dy} \frac{\partial}{\partial m} = -\eta \frac{\partial}{\partial m} \tag{19}$$

in which we have used the fact that the absolute vorticity $\eta = -\partial_y m$. Using this transformation, the relative vorticity ζ becomes

$$\zeta = -\frac{\partial u}{\partial y} = \eta \frac{\partial u}{\partial m}, \tag{20}$$

and the definition of absolute vorticity allows ζ to be written

$$\zeta = \frac{\beta y \frac{\partial u}{\partial m}}{1 - \frac{\partial u}{\partial m}}. \tag{21}$$

This serves as our indicator of the formation of a true front: ζ becomes singular when $\partial_m u$ increases to unity. Note that for $\partial_m u > 1$, m is no longer monotonic in y and so the use of the definition of m as a coordinate mapping breaks down.

The central part of this derivation involves writing a form of the thermal wind equation and then showing how WISHE and other processes modify the sharpness and meridional position of zonal wind gradients via the free-tropospheric temperature field. The thermal wind relation can be written in terms of m :

$$\beta y \frac{\partial m}{\partial p} = \frac{\partial s^*}{\partial y} \left(\frac{\partial T}{\partial p} \right)_{s^*}, \quad (22)$$

where the derivative of T is taken on an s^* surface. This expression and the following treatment are not specific to the two-mode model, in that no modal decomposition is used. The only assumptions made thus far are those of axisymmetry and thermal wind balance. Now we also assume that the atmosphere is neutral to slantwise convection, so that s^* surfaces are parallel to m surfaces. Then, applying the chain rule to the right-hand side of (22) and dividing through by $\partial_y m$ provides an expression for the slope of an m surface:

$$\beta y \left(\frac{\partial y}{\partial p} \right)_m = - \frac{ds^*}{dm} \left(\frac{\partial T}{\partial p} \right)_{s^*}. \quad (23)$$

This expression is integrated upward along s^* and m surfaces:

$$\frac{ds^*}{dm} (T_s - T) = \frac{\beta}{2} y^2 \Big|_m = u - u_s, \quad (24)$$

which is simply a discretized form of thermal wind balance in m space. The last expression on the right was obtained using the definition of m and represents the vertical shear of zonal wind along an m surface, with u_s the wind at the lower boundary of the atmosphere. For a hurricane, E97 obtained ds^*/dm solely in terms of m and u_s by virtue of the fact that m surfaces flare out to a large radius at the top of the storm and by the assumption that the contribution of u_s to m is much larger than that of the planetary rotation. These extremes do not apply to the monsoonal regime considered here. However, we exploit the baroclinic nature of the circulation by evaluating (24) at the level at which the zonal wind vanishes:

$$\Delta T_0 \frac{ds^*}{dm} = -u_s, \quad (25)$$

where ΔT_0 is defined as the difference between the surface temperature T_s and the temperature at the level

of zero zonal wind. If the circulation has a nonzero barotropic component, then $\Delta T_0 \neq T_s - \bar{T}$, with \bar{T} being the pressure-weighted mean tropospheric temperature. Indeed, a level of zero zonal wind may not exist given a sufficiently strong barotropic wind, although this is generally not the case in monsoon climates in which low-level westerlies occur together with upper-level easterlies. This adds some precision to the preceding heuristic assumption that the tendency of s^* due to WISHE will be proportional to the magnitude of the baroclinic zonal wind. We proceed with the analysis with the awareness that time variations in ΔT_0 (i.e., in the level of zero zonal wind) could alter the behavior.

The time evolution of u in m space can be obtained by differentiating the linearized free-tropospheric temperature balance with respect to m :

$$\frac{\partial^2 s^*}{\partial m \partial t} = \frac{\partial}{\partial m} [N^2 (\varepsilon M_c - w)]. \quad (26)$$

We assume that the convective mass flux M_c instantaneously adjusts to the value needed to maintain constant subcloud-layer entropy:

$$M_c = M_{\text{eq}} \equiv w + \frac{1}{\chi} \left(C_{\kappa} |\mathbf{V}| \gamma + H_b \alpha u_s \frac{\partial s_b}{\partial m} \right), \quad (27)$$

where the quantities $\chi \equiv s_b - s_m$ and $\gamma \equiv s_o^* - s_b$ are not necessarily constants here. The advective tendency of s_b has been written in m coordinates, using the fact that the only meridional wind in m space, v_m , is that induced by surface friction, here represented by Rayleigh damping:

$$v_m \equiv \frac{Dm}{Dt} = -\alpha u_s. \quad (28)$$

Using this closure for M_c together with (25) gives

$$\begin{aligned} \frac{\partial}{\partial t} \left(\frac{u_s}{\Delta T_0} \right) = N^2 \Bigg[& - \frac{\varepsilon C_{\kappa} \gamma}{\chi |\mathbf{V}|} \left(\frac{\partial u_s}{\partial m} + \frac{\partial v_s}{\partial m} \right) - \varepsilon C_{\kappa} |\mathbf{V}| \frac{\partial}{\partial m} \left(\frac{\gamma}{\chi} \right) \\ & - \varepsilon \frac{\partial}{\partial m} \left(\frac{H_b \alpha u_s}{\chi} \frac{\partial s_b}{\partial m} \right) + (1 - \varepsilon) \frac{\partial w}{\partial m} \Bigg]. \quad (29) \end{aligned}$$

The first and third terms on the right-hand side will generally increase u_s by enhancing meridional gradients of s^* . The first term represents the effect of WISHE and the third term indicates the effect of meridional advection of subcloud-layer entropy. If we neglect the contribution of the meridional wind to the wind-

induced surface entropy flux and also eliminate $\partial_m s_b$ using (25) then, following E97, these two terms can be seen to propagate the u_s distribution meridionally with a phase speed given by

$$c = \frac{\varepsilon N^2}{\chi} \left[\frac{\Delta T_0 C_\kappa \gamma}{|\mathbf{V}|} - \frac{2H_b \alpha}{\Delta T_0} u_s \right]. \quad (30)$$

The first term in brackets results from WISHE and is positive; it thus propagates the u_s distribution toward higher m (i.e., lower y). Because the equatorward phase speed varies inversely with $|\mathbf{V}|$, meridional gradients of u_s will be enhanced on the poleward side of the peak surface wind speed and reduced on the equatorward side of this peak. When $\partial_m u_s$ increases to unity, (21) shows that a front will exist. The second term in brackets in (30) is due to s_b advection and is negative; it propagates the u_s distribution toward lower m , in the opposite direction of the WISHE term. However, this term is also frontogenetic because it increases $\partial_m u_s$ on the poleward side of the u_s peak (because the poleward phase speed due to s_b advection increases with u_s). Performing this analysis in m space shows that it is the meridional wind due to surface drag that is responsible for the frontogenetic tendency of this term: surface drag produces boundary layer flow that advects lower values of s_b toward the s_b peak, thus packing s^* surfaces closer together under the assumption of subcloud quasi-equilibrium.

The second and fourth terms on the right-hand side of (29) damp frontogenesis by reducing meridional gradients of s^* . The second term represents the tendency of surface entropy fluxes to relax the s_b distribution toward the specific entropy of the ocean surface, preventing s_b gradients from becoming sharper than those of the lower boundary entropy. The fourth term represents the tendency of vertical velocities in a thermally direct circulation to adiabatically reduce the horizontal temperature gradients that drive the circulation. Although the above development does not address the nature of the equilibrium achieved between the four terms on the right-hand side of (29), the two-mode model runs in which WISHE and s_b advection were selectively omitted confirm that those two processes do shift the u_s maximum toward the equator and the pole, respectively (as seen in the shifts of s_b shown in Fig. 8, discussed above). It is difficult to discern any considerable increase in $\partial_y u_s$ on the poleward side of the u_s peak in the two-mode model caused by either WISHE or s_b advection because this gradient is already large simply because of the sharp northern boundary of the Hadley circulation. Thus, our focus is on meridional propaga-

tion rather than the associated frontogenesis, although we henceforth refer to the physics responsible for this propagation as the frontogenetic mechanism and recognize that it might have broader application in tropical dynamics.

The two-mode model used in this paper has a vertical structure simplified by the assumption that variations in s^* are constant with height. This simplification involved taking the thermal wind relation

$$\beta y \frac{\partial u}{\partial p} = \frac{\partial s^*}{\partial y} \left(\frac{\partial T}{\partial p} \right)_{s^*} \quad (31)$$

and integrating it along an s^* surface to obtain

$$\beta y (u - u_s) = (T - T_s) \frac{\partial s^*}{\partial y}. \quad (32)$$

This last step assumes that $\partial_y s^*$ is constant along s^* surfaces, which is generally true only if s^* surfaces are vertical (i.e., parallel to y surfaces). Thus, the two-mode model assumes that s^* and m surfaces are not parallel; the former are vertical whereas the latter are tilted in this model.

The expression (29) derived for a slantwise neutral fluid would thus seem to be inapplicable to the two-mode model. However, a similar procedure can be followed in physical space, rather than m space, to obtain

$$\begin{aligned} \frac{\partial^2 s^*}{\partial t \partial y} = \frac{1}{\beta y \Delta T} \frac{\partial u_s}{\partial t} = N^2 \left[\varepsilon C_\kappa \frac{\gamma}{\chi |\mathbf{V}|} \left(\frac{\partial u}{\partial y} + \frac{\partial v}{\partial y} \right) \right. \\ \left. + \varepsilon C_\kappa |\mathbf{V}| \frac{\partial}{\partial y} \left(\frac{\gamma}{\chi} \right) - \varepsilon \frac{\partial}{\partial y} \left(\frac{Hv \partial s_b}{\chi \partial y} \right) - (1 - \varepsilon) \frac{\partial w}{\partial y} \right]. \end{aligned} \quad (33)$$

The WISHE and advective terms here also increase gradients of u_s on the poleward side of the surface wind maximum, but $\partial_y u$ must become singular for the relative vorticity to become singular. This means that it takes infinite time to form a discontinuity in u by (33), consistent with the fact that nonlinear u advection was not used to derive (33). Thus, although the slantwise neutral solution (29) is not strictly applicable to the two-mode model, the mechanisms that produce velocity fronts in this model seem similar. The two-mode model may even approximate the nonlinear momentum advection needed to achieve the faster frontogenetic rates of the m -conserving, slantwise neutral solution.

5. Results for equatorial forcings

a. Steady forcings

Thermal forcings with a first or second meridional derivative that is nonzero on the equator are expected

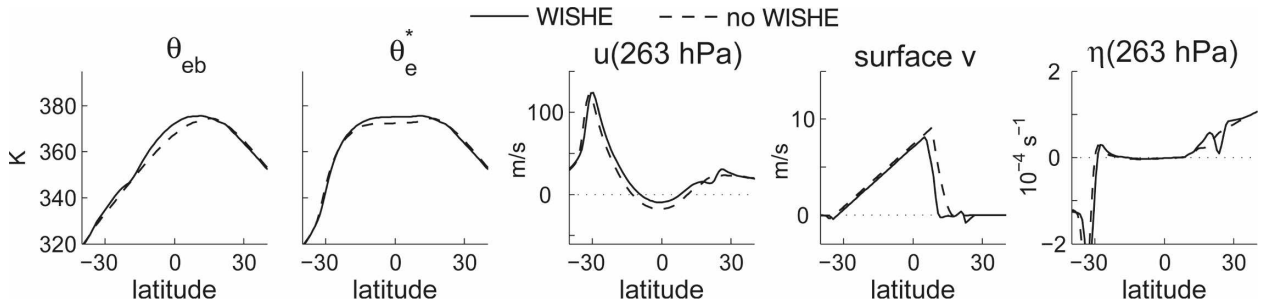


FIG. 9. As in Fig. 2, but for the equilibrated response to the steady T_{LH} forcing centered at $\phi_1 = 10^\circ\text{N}$.

to produce an AMC circulation regardless of the magnitude of the forcing, as discussed by Plumb and Hou (1992). For such forcings, m conservation is expected to constrain the dynamics as it did for the subtropical forcings, although we find that there are a few features worth noting. For this reason, the two-mode model is integrated with the T_{LH} forcing given in (7), with $T_1 = 303.15\text{ K}$ and $\theta_{\text{LH}} = 20\text{ K}$. We examine several values of ϕ_1 , the latitude of the SST maximum.

For an SST maximum at $\phi_1 = 10^\circ\text{N}$, a cross-equatorial AMC circulation is produced that extends to nearly 40°S , regardless of whether WISHE is included in the model (Fig. 9). Convection is suppressed in the winter hemisphere branch of the circulation, where $s^* > s_b$. Consistent with the results for subtropical forcings, the ascent zone is narrower and located closer to the equator in the run with WISHE than in the run without (dashed lines in Fig. 10). The fact that upper-level zonal winds are slightly more westerly in the run with WISHE is consistent with this equatorward shift in ascent.

For an equatorially symmetric forcing with $\phi_1 = 0$, a single ascent peak exists on the equator only when WISHE is not included (Fig. 10). The use of WISHE produces two ascent zones symmetric about the equator, with a local minimum in ascent on the equator. This same effect of wind-dependent ocean evaporation was obtained by Numaguti (1993) in a three-dimensional aquaplanet GCM with a zonally symmetric SST prescribed to peak on the equator, and we present a brief discussion consistent with his explanation of the underlying physics. As shown by Held and Hou (1980), to balance the divergence of zonal momentum produced by an AMC response with ascent peaking on the equator, surface winds must consist of easterlies between the equator and some intermediate latitude, westerlies poleward of this latitude, and zero wind on the equator in the inviscid, nondiffusive limit. With WISHE, however, this surface wind distribution is incompatible with an equatorial peak of free-tropospheric temperatures, as can be seen by differentiating the steady-state ver-

sion of the budget for s^* , under the assumption of strict subcloud-layer quasi-equilibrium:

$$0 = \frac{\partial}{\partial y} \left[-\frac{\varepsilon}{\chi} E - \frac{\varepsilon H_b}{\chi} v \frac{\partial s_b}{\partial y} + (1 - \varepsilon)w + \frac{R}{N^2} \right]. \quad (34)$$

For an equatorial SST peak without WISHE, peak ascent is maintained on the equator because surface entropy fluxes peak there, and the positive first term and negative third term in the above expression roughly balance. For an equatorial SST peak with WISHE, the fact that m conservation requires a local minimum in $|\mathbf{V}|$ on the equator means that the first term in (34) will become negative, unless gradients in χ or $(s_b^* - s_b)$ are sufficiently large to compensate for the poleward gradient in $|\mathbf{V}|$. Although χ is fixed in the two-mode model,

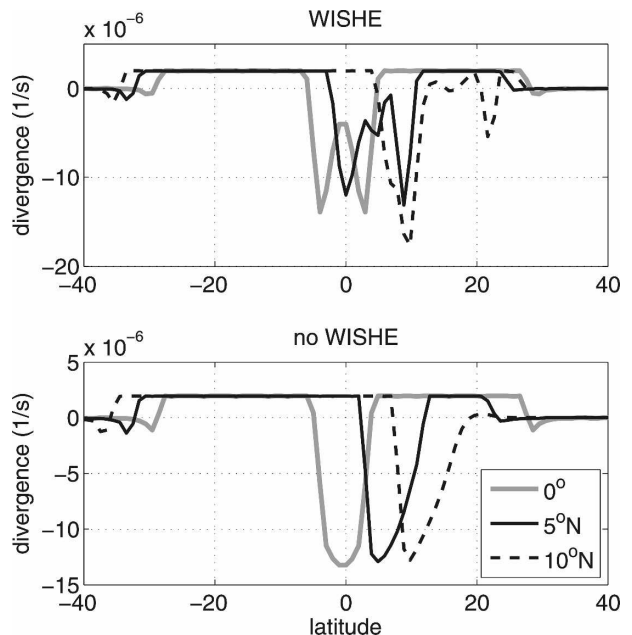


FIG. 10. Surface divergence for the equilibrated response to the steady T_{LH} forcing centered at 0° (gray solid line), 5°N (black solid line), and 10°N (dashed line): results for the runs (top) with and (bottom) without WISHE.

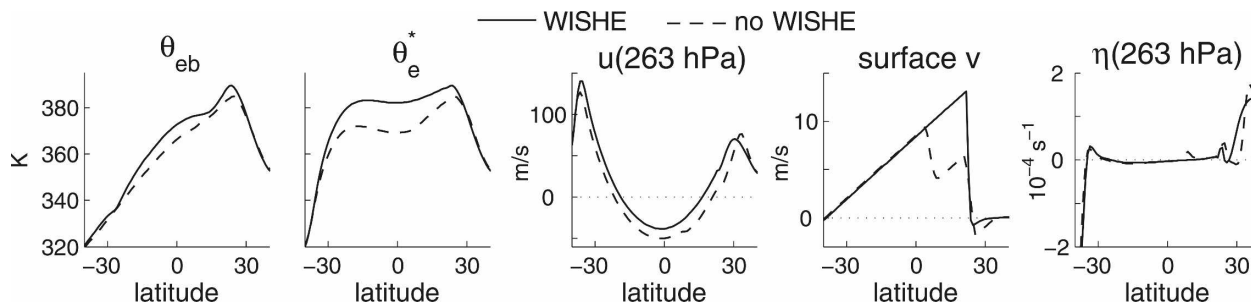


FIG. 11. As in Fig. 9, but for the equilibrated response to the steady T_C forcing (the combination of the T_{PH} and T_{LH} forcings).

its variations could produce a moisture–convection feedback (e.g., Grabowski and Moncrieff 2004) in which the convective mass flux increases as the lower free-troposphere moistens. We do not explore this further here but simply note that this is one candidate mechanism for maintaining maxima in convection and ascent on the equator when E has a local minimum there. Advection of s_b , represented by the second term in (34), is another such candidate, but this advective tendency should be quite weak near the equator because of the flatness of the m -conserving distribution of s_b there. A poleward gradient in the radiative cooling R is another candidate for preserving an equatorial maximum in w , and such a gradient would be consistent with reduced longwave cooling due to cloudiness on the equator. Thus, if variations in χ , R , or the advection of s_b do not compensate, the poleward gradient in E near the equator that is produced by WISHE must be balanced by a poleward gradient in w . Alternatively, the energy budget of the ocean mixed layer could play a role in maintaining both a precipitation maximum and an evaporation minimum on the equator, as discussed by both Sobel (2003) and Seager et al. (2003). Indeed, results from those studies suggest that splitting of the convergence zone by WISHE may occur only when SST is fixed.

By similar arguments to those presented for an equatorial SST maximum, a bimodal profile of w with a near-equatorial local minimum is expected to exist for SST distributions that peak very near, though not precisely on, the equator. This is seen in the two-mode model, where a northward shift of ϕ_1 from the equator to 5°N produces a similar northward shift in the two ascent zones (Fig. 10). This is consistent with the results of Lindzen and Hou (1988), in that the peak surface easterlies in the winter hemisphere tropics of their dry model moved toward the equator as the forcing maximum was shifted off the equator into the summer hemisphere. The surface easterly peak in the winter hemisphere is expected to be associated with a local maximum of ascent until the thermally direct circulation is

strong enough to suppress convection in the winter trade wind region.

Although this shift of the ascent zone off the equator for near-equatorial forcings may seem to contradict the previous statement that WISHE shifts ascent zones toward the equator, it is not at odds with the frontogenetic mechanism. That mechanism can be viewed as simply having a lower bound for the latitude of the s^* peak. That is, if the SST peak were to be moved quasi-statically from the subtropics to the equator, the equatorially symmetric peaks of the m -conserving s^* distribution would move toward the equator until they reached some limiting latitude. These s^* peaks would only move onto the equator if the meridional gradient of the surface entropy flux between the peaks became zero, a process that WISHE prevents from occurring. It is worth noting that for SSTs peaking on or very near the equator, the frontogenetic mechanism must take into account the possibility that easterlies may exist at all heights near the ascent zone so that no level of zero zonal wind exists.

We now examine the response to a forcing that contains both cross-equatorial and subtropical components, represented by T_C in (8). To our knowledge, this combination of an idealized cross-equatorial forcing with a subtropical forcing has not been explored even in axisymmetric dry models. The subtropical SST anomaly is given an amplitude of $\theta_{PH} = 2$ K, which for the isolated subtropical forcing of T_{PH} was supercritical only with the effects of WISHE. The response to T_C largely seems to be a superposition of the responses to the individual components of the forcing (T_{LH} and T_{PH}) with the AMC circulation dominating wherever it exists. That is, for the run with WISHE, ascent occurs only in a narrow zone just south of the subtropical SST maximum, and no ascent occurs near the equator despite the nonzero cross-equatorial gradients of both SST and s_b (Fig. 11). The main effect of the T_{LH} component of the forcing is to extend the poleward boundary of the AMC circulation to higher latitudes in the winter hemisphere (cf. Fig. 11 with the second row of Fig. 2). In the run

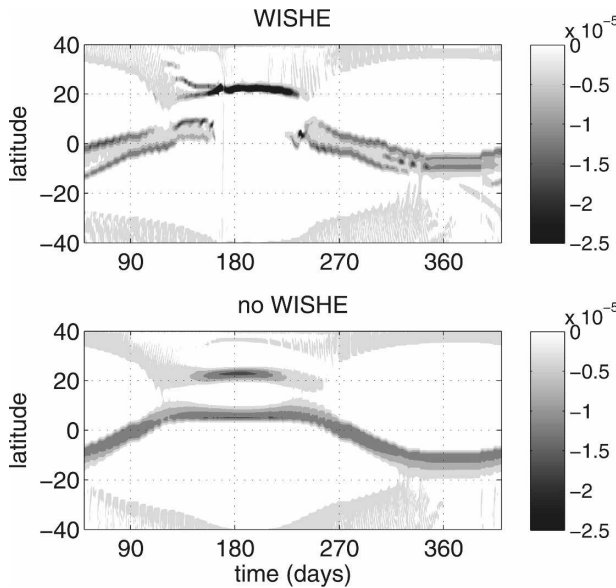


FIG. 12. Hovmöller diagrams of surface divergence, in units of s^{-1} , for the response to the seasonally varying combined forcing (see text for the form of the forcing) for the runs (top) with and (bottom) without WISHE. Time is the number of days after the boreal winter solstice.

without WISHE, the subtropical component of the forcing does not generate a cross-equatorial AMC response, so ascent occurs both near $20^{\circ}N$ and just north of the equator due to the equatorial component of the forcing.

b. Seasonally varying forcings

Finally, this combined forcing is varied in a seasonal cycle, which can be thought of as an idealization of seasonal variations both in SST and in the thermal forcing associated with an off-equatorial landmass in a monsoon climate. This seasonal variation is accomplished by using T_C in (8) as the forcing but prescribing ϕ_1 in (7) and θ_{PH} in (6) to vary in phase with the same annual frequency:

$$\phi_1 = 10^{\circ} \cos\left(2\pi \frac{t}{365 \text{ days}}\right), \quad \text{and} \quad (35)$$

$$\theta_{PH} = 2 \text{ K} \cos\left(2\pi \frac{t}{365 \text{ days}}\right). \quad (36)$$

At any point in the resulting seasonal cycle, the response is generally consistent with the steady results discussed above. In the run without WISHE, ascent occurs both near the equator and near the subtropical SST peak during boreal summer (Fig. 12, bottom panel). The near-equatorial ascent zone migrates back and forth across the equator in a continuous annual

cycle and is confined closer to the equator in boreal summer than in boreal winter because of subsidence forced by the subtropical SST anomaly.

In the run with WISHE, ascent occurs only near $20^{\circ}N$ at the boreal summer solstice (Fig. 12, top panel), as it did in the equilibrated response to the steady combined forcing. During spring and fall, a region of ascent migrates across the equator, but within this region a local minimum of ascent exists between two maxima positioned on opposite sides of the equator. Again, this is consistent with the steady response to the T_{LH} forcing when the SST maximum was located on or near the equator. During the transition from spring to summer, the ascent zone jumps discontinuously from its near-equatorial position to the location just south of the subtropical SST peak. This jump is a signature of the transition to an AMC circulation forced by the subtropical SST peak, and WISHE simply causes this transition to occur when θ_{PH} peaks at the intermediate amplitude of 2 K. That is, a similar jump occurs even without WISHE if θ_{PH} is increased to 5 K, although the use of WISHE makes the jump occur earlier in the seasonal cycle (not shown).

6. Concluding remarks

The effect of WISHE on axisymmetric Hadley circulations can be summarized by considering four different regimes. For the weakest SST forcings localized off the equator, WISHE only mildly enhances the strength of the circulation because surface drag suppresses its positive feedback on the baroclinic component of the circulation. For slightly stronger SST forcings, the convergence of zonal momentum into the off-equatorial ascent zone can overcome the damping effects of surface drag, allowing WISHE to more strongly enhance the sensitivity of the circulation strength to the forcing. These are the two cases discussed by BE08, and upper tropospheric meridional flow does not homogenize absolute angular momentum in either of these regimes.

For stronger SST forcings, WISHE can cause the circulation to enter an AMC regime when, in the absence of WISHE, only a local, viscous response would be produced. That is, WISHE reduces the critical forcing needed to produce an AMC response. This reduction in the forcing threshold was shown to occur because of a mechanism similar to that thought responsible for the frontal collapse of hurricane eyewalls (i.e., an adaption of the theory of E97). For forcings strong enough to produce AMC flow even in the absence of WISHE, the conservation of angular momentum was shown to provide a strong dynamical constraint. The primary effect of WISHE for such strong forcings was the same slight

narrowing and equatorward shift of the ascent zone and the subcloud entropy peak that occurred for weaker forcings. All of these results were shown to hold for seasonally varying forcings, so that when the strongest SST forcings were varied in a seasonal cycle, WISHE shifted the abrupt onset to a time earlier in the seasonal cycle. For weaker seasonally varying forcings that would not produce AMC flow in the absence of WISHE, WISHE produced an abrupt onset either by reducing the critical threshold for an AMC response or, as shown in BE08, by providing a positive feedback on the strength of non-AMC flow.

These results hold even when the SST has a nonzero gradient on equator. That is, when a subtropical forcing is superimposed on an SST distribution with a cross-equatorial gradient, the origin of the m -conserving flow can be shifted from the equator nearly into the subtropics, thereby suppressing any near-equatorial convection. This shift in the origin of the m -conserving flow occurs once the subtropical forcing exceeds the threshold discussed by Plumb and Hou (1992), which shows that the criticality condition is relevant even when AMC flow already occurs in some other part of the domain. This suggests that strong near-equatorial SST gradients may have little effect on the Hadley circulation given a sufficiently strong forcing associated with an off-equatorial landmass.

It is not obvious where the earth's zonal-mean Hadley circulation or regional monsoon circulations lie in the series of regimes just discussed. That is, are the thermal forcings associated with the off-equatorial landmasses in monsoon climates sufficiently strong to produce AMC flow in the absence of WISHE? If the axisymmetric model used in this paper does represent the physics responsible for setting meridional flow in, say, the South Asian monsoon, the fact that a secondary ascent zone exists just south of the equator in the Indian Ocean in the boreal summer mean might indicate that the thermal forcings in this region are subcritical or only marginally supercritical, even with WISHE. If the South Asian monsoon does exist in such a marginal state, fairly small reductions in the amplitude of the off-equatorial thermal forcing—say, due to changes in orography or land surface albedo in past or future climates—could shift the system into a different regime and greatly change rainfall patterns in the region.

The question of whether WISHE plays an important role in the abrupt onset of the South Asian monsoon might be largely separate from the question of what sets the state of the mean summer monsoon. It was shown by BE08 that a WISHE feedback can produce an abrupt onset even for subcritical forcings. And even if the damping effects of interactive SST prove strong

enough to eliminate all effects of WISHE for an equilibrated response, the ocean time scales may be sufficiently slow so as to permit WISHE to act in a transient sense during monsoon onset. Such a transient effect would be consistent with measurements of ocean evaporation collected over the course of 1 yr from a surface mooring deployed in the Arabian Sea along the climatological axis of the southwesterly Somali jet (Weller et al. 1998). In that study, ocean evaporation peaked shortly after the onset of the southwesterly jet, then decreased as the summer monsoon season progressed due to both a reduction in SST and an increase in the relative humidity of surface air over the Arabian Sea.

The models used in this paper did not include the effects of numerous processes that could qualitatively change the results, including zonal asymmetries, interactive SST, land surface hydrology, and moisture–radiation feedbacks. It would be especially intriguing to see how use of a prognostic dynamical boundary layer alters the results because Bellon and Sobel (2008) found that boundary layer effects were important in their simulation of meridionally propagating convective anomalies that were destabilized by WISHE. Yet even without exploring the possible importance of all of these processes in models, it may be possible to assess the consistency of observations with some features of the theoretical ideas presented here, thereby providing evidence for or against the role of WISHE in the onset of monsoons. This task will be undertaken in a separate work.

Acknowledgments. The research presented here constituted part of the first author's doctoral thesis and was supported by the National Science Foundation under Grant ATM-0432090. Thoughtful comments by Adam Sobel and an anonymous reviewer improved this manuscript.

APPENDIX A

On Secondary, Near-Equatorial Convergence Zones

Solstitial Hadley circulations generally consist of a narrow, off-equatorial region of low-level convergence and a meridionally broad region of weak subsidence that stretches across the equator into the winter hemisphere (e.g., Lindzen and Hou 1988; Plumb and Hou 1992). In the two-mode model, however, a secondary ascent zone was sometimes found on the winter side of the equator (e.g., for the response without WISHE to the steady subtropical forcing with $\theta_{PH} = 4$ K, seen in

the bottom row of Fig. 2). Within this secondary ascent zone, the equatorial minimum of the m -conserving distribution of s^* is not elevated above the subcloud entropy s_b . If s^* dips below s_b , convection will occur, heating the free troposphere and creating a pressure gradient that drives local ascent. The equatorial minimum of s^* might thus provide one explanation for the existence of the secondary, near-equatorial ascent zone, although it does not explain why the secondary ascent zone is located on the winter side of the equator.

A more detailed explanation was given by Pauluis (2004), who showed that a secondary ascent zone can exist on the winter side of the equator for solstitial Hadley circulations when equatorial boundary layer temperature gradients are insufficient to maintain cross-equatorial flow against surface drag. Although the two-mode model does not possess a dynamical boundary layer, similar reasoning applies because projection of the full momentum equations onto two modes effectively distributes surface drag through the depth of the entire troposphere. The projected, steady-state meridional momentum equation is (from BE08):

$$Cv_1 \frac{\partial v_1}{\partial y} = \frac{\partial s^*}{\partial y} - \beta y u_1 - \frac{C_D |\mathbf{V}|}{H \langle T'^2 \rangle} v_1, \quad (\text{A1})$$

where the constant C results from the projection operation and is given in terms of various moments of the vertical structure function:

$$C = \frac{\langle T'^3 \rangle}{\langle T'^2 \rangle} - \frac{\langle \Omega T' \partial_p T' \rangle}{\langle T'^2 \rangle}. \quad (\text{A2})$$

For the vertical structures considered here, C is negative. If the nonlinear advective term on the left-hand side is neglected, which was the case considered by Pauluis (2004), a cross-equatorial gradient of s^* is needed to maintain flow against friction on the equator. Pauluis (2004) showed that an upper bound on meridional wind also exists off the equator and that this upper bound is higher on the winter side of the equator than on the summer side. This asymmetry in the upper bound requires the reduction in v , and thus the ascent, to occur on the winter side of the equator.

A similar equatorial asymmetry on the bounds of v_1 occurs in the two-mode model, although it can be explained using somewhat different logic. The cross-equatorial Hadley cell in this model is thermally direct, so u_1 and v_1 will generally have the same sign within the cross-equatorial Hadley cell (u_1 is the baroclinic component of zonal wind, and in boreal summer it is generally positive on and near the equator even when the total surface wind is easterly there). The vertically integrated Coriolis torque will then oppose surface drag

in the winter hemisphere but augment surface drag in the summer hemisphere. This results in a larger upper bound on v_1 in the winter hemisphere, as in Pauluis (2004). The two-mode model also has the convenient property that the left-hand side of (A1) contains the full nonlinear advective term for the meridional momentum balance. In subsiding regions, $v_1 \partial_y v_1 > 0$, so this advective term, although it might be quite small, will oppose surface drag (because $C < 0$) and act to maintain cross-equatorial flow. This provides another reason for the secondary ascent zone to occur on the winter side of the equator, because there the negative tendencies of nonlinear advection and surface drag in the secondary ascent zone can be balanced by the Coriolis torque. The secondary ascent zone cannot occur on the summer side of the equator because there the weak meridional gradients of s^* alone would have to balance the combined negative tendencies of Coriolis torque, surface drag, and nonlinear advection of meridional momentum.

Although the secondary ascent zone was only shown for the one run without WISHE for $\theta_{\text{PH}} = 4$ K, it was a robust feature of the model that occurred for many forcings of intermediate strength not shown in the plots presented here. That is, as a steady subtropical forcing was increased in amplitude, the circulation transitioned from a local, viscously dominated circulation to an m -conserving circulation with a secondary ascent zone on the winter side of the equator and finally to an m -conserving circulation with subsidence stretching continuously across the equator.

APPENDIX B

Angular Momentum–Conserving Temperature in the Two-Mode Model

The free-tropospheric temperature needed to balance winds that conserve absolute angular momentum near the tropopause was shown by Plumb and Hou (1992) to be a critical distribution in the steady, inviscid limit: when the horizontal curvature of temperature exceeds that of this critical distribution, a thermally direct circulation must exist. This critical distribution was phrased in terms of subcloud-layer entropy for an atmosphere in convective quasi-equilibrium by Emanuel (1995). However, the distribution of Emanuel (1995) cannot be rephrased on a β plane and directly applied to the two-mode model because this model only conserves absolute angular momentum at one particular level slightly below its specified tropopause, as discussed in section 2a. Burns et al. (2006) showed that the m -conserving baroclinic zonal wind can be obtained

simply by integrating the expression for m conservation at this level. This is done by using the fact that $u_0 = -u_1$ to first order in their asymptotic expansion, so that (11) can be rewritten, for nonzero v_1 , as

$$(A - 1) \frac{\partial u_1}{\partial y} = \beta y. \quad (\text{B1})$$

As also noted by Burns et al. (2006), the free-tropospheric temperature can be obtained by assuming geostrophic balance:

$$\beta y u_1 = \Delta T \frac{\partial s^*}{\partial y}. \quad (\text{B2})$$

If (B1) is integrated from the latitude of maximum s^* , denoted y_m , and that result is used in integrating (B2) from the same latitude, the result is

$$s^* = s_m^* - \frac{\beta^2}{8\Delta T(A - 1)} (y_m^2 - y^2)^2. \quad (\text{B3})$$

Here, s_m^* is the maximum saturation entropy in the free troposphere (at latitude y_m) and s^* is the saturation entropy at latitude y . Using the definition $s \equiv c_p \ln \theta_e$ and the assumption that $s^* = s_b$ in convective quasi-equilibrium, this provides an expression for the critical distribution of the subcloud-layer equivalent potential temperature θ_{eb} in the two-mode model:

$$\theta_{eb} = \theta_{em} \exp[-\xi(y_m^2 - y^2)^2], \quad (\text{B4})$$

with the constant ξ given by

$$\xi = \frac{\beta^2}{8c_p \Delta T(A - 1)}. \quad (\text{B5})$$

Here, θ_{em} is the peak equivalent potential temperature of the subcloud layer (at latitude y_m).

REFERENCES

- Bellon, G., and A. H. Sobel, 2008: Poleward-propagating intraseasonal monsoon disturbances in an intermediate-complexity axisymmetric model. *J. Atmos. Sci.*, **65**, 470–489.
- Boos, W. R., and K. A. Emanuel, 2008: Wind–evaporation feedback and abrupt seasonal transitions of weak, axisymmetric Hadley circulations. *J. Atmos. Sci.*, **65**, 2194–2214.
- Burns, S., A. H. Sobel, and L. Polvani, 2006: Asymptotic solutions of the axisymmetric moist Hadley circulation in a model with two vertical modes. *Theor. Comput. Fluid Dyn.*, **20**, 443–467.
- Emanuel, K. A., 1995: On thermally direct circulations in moist atmospheres. *J. Atmos. Sci.*, **52**, 1529–1534.
- , 1997: Some aspects of hurricane inner-core dynamics and energetics. *J. Atmos. Sci.*, **54**, 1014–1026.
- Frierson, D., A. Majda, and O. Pauluis, 2004: Large-scale dynamics of precipitation fronts in the tropical atmosphere: A novel relaxation limit. *Comm. Math. Sci.*, **2** (4), 591–626.
- Grabowski, W. W., and M. W. Moncrieff, 2004: Moisture–convection feedback in the tropics. *Quart. J. Roy. Meteor. Soc.*, **130**, 3081–3104.
- Halpern, D., and P. M. Woiceshyn, 1999: Onset of the Somali Jet in the Arabian Sea during June 1997. *J. Geophys. Res.*, **104**, 18 041–18 046.
- Held, I. M., and A. Y. Hou, 1980: Nonlinear axially symmetric circulations in a nearly inviscid atmosphere. *J. Atmos. Sci.*, **37**, 515–533.
- Krishnamurti, T. N., P. Ardanuy, Y. Ramanathan, and R. Pasch, 1981: On the onset vortex of the summer monsoon. *Mon. Wea. Rev.*, **109**, 344–363.
- Lau, W., and D. Waliser, Eds., 2005: *Intraseasonal Variability in the Atmosphere–Ocean Climate System*. Springer, 436 pp.
- Lindzen, R. S., and A. Y. Hou, 1988: Hadley circulation for zonally averaged heating centered off the equator. *J. Atmos. Sci.*, **45**, 2416–2427.
- Murakami, T., L.-X. Chen, and A. Xie, 1986: Relationship among seasonal cycles, low-frequency oscillations, and transient disturbances as revealed from outgoing longwave radiation data. *Mon. Wea. Rev.*, **114**, 1456–1465.
- Neelin, J. D., and N. Zeng, 2000: A quasi-equilibrium tropical circulation model—Formulation. *J. Atmos. Sci.*, **57**, 1741–1766.
- Numaguti, A., 1993: Dynamics and energy balance of the Hadley circulation and the tropical precipitation zones: Significance of the distribution of evaporation. *J. Atmos. Sci.*, **50**, 1874–1887.
- , 1995: Dynamics and energy balance of the Hadley circulation and the tropical precipitation zones. Part II: Sensitivity to meridional SST distribution. *J. Atmos. Sci.*, **52**, 1128–1141.
- Pauluis, O., 2004: Boundary layer dynamics and cross-equatorial Hadley circulation. *J. Atmos. Sci.*, **61**, 1161–1173.
- , and K. Emanuel, 2004: Numerical instability resulting from infrequent calculation of radiative heating. *Mon. Wea. Rev.*, **132**, 673–686.
- Peixoto, J. P., and A. H. Oort, 1992: *Physics of Climate*. American Institute of Physics, 520 pp.
- Plumb, R. A., and A. Y. Hou, 1992: The response of a zonally symmetric atmosphere to subtropical thermal forcing: Threshold behavior. *J. Atmos. Sci.*, **49**, 1790–1799.
- Privé, N. C., and R. A. Plumb, 2007: Monsoon dynamics with interactive forcing. Part I: Axisymmetric studies. *J. Atmos. Sci.*, **64**, 1417–1430.
- Raymond, D. J., 1995: Regulation of moist convection over the West Pacific warm pool. *J. Atmos. Sci.*, **52**, 3945–3959.
- Schneider, T., and S. Bordoni, 2008: Eddy-mediated regime transitions in the seasonal cycle of a Hadley circulation and implications for monsoon dynamics. *J. Atmos. Sci.*, **65**, 915–934.
- Seager, R., R. Murtugudde, A. Clement, and C. Herweijer, 2003: Why is there an evaporation minimum at the equator? *J. Climate*, **16**, 3793–3802.
- Sobel, A., 2003: On the coexistence of an evaporation minimum and precipitation maximum in the warm pool. *J. Climate*, **16**, 1003–1009.
- , and J. Neelin, 2006: The boundary layer contribution to intertropical convergence zones in the quasi-equilibrium tropical circulation model framework. *Theor. Comput. Fluid Dyn.*, **20**, 323–350.
- Walker, C. C., and T. Schneider, 2006: Eddy influences on Hadley circulations: Simulations with an idealized GCM. *J. Atmos. Sci.*, **63**, 3333–3350.
- Wang, B., 2006: *The Asian Monsoon*. Springer, 787 pp.
- Webster, P. J., V. O. Magaña, T. N. Palmer, J. Shukla, R. A.

- Tomas, M. Yanai, and T. Yasunari, 1998: Monsoons: Processes, predictability, and the prospects for prediction. *J. Geophys. Res.*, **103**, 14 451–14 510.
- Weller, R. A., M. F. Baumgartner, S. A. Josey, A. S. Fischer, and J. C. Kindle, 1998: Atmospheric forcing in the Arabian Sea during 1994–1995: Observations and comparisons with climatology and models. *Deep-Sea Res.*, **45**, 1961–1999.
- Wirth, V., and T. J. Dunkerton, 2006: A unified perspective on the dynamics of axisymmetric hurricanes and monsoons. *J. Atmos. Sci.*, **63**, 2529–2547.
- Yasunari, T., 1979: Cloudiness fluctuations associated with the Northern Hemisphere summer monsoon. *J. Meteor. Soc. Japan*, **57**, 227–242.
- Zeng, N., J. Neelin, and C. Chou, 2000: A quasi-equilibrium tropical circulation model: Implementation and simulation. *J. Atmos. Sci.*, **57**, 1767–1796.